European Journal of Pharmaceutical Sciences xxx (2014) xxx–xxx

Contents lists available at ScienceDirect

European Journal of Pharmaceutical Sciences

journal homepage: www.elsevier.com/locate/ejps

Identification of new 4-*N*-substituted 6-aryl-7*H*-pyrrolo[2,3-*d*] pyrimidine-4-amines as highly potent EGFR-TK inhibitors with Src-family activity

Svein Jacob Kaspersen [a], Jin Han [a,b], Kristin G. Nørsett [c], Line Rydså [a,1], Eli Kjøbli [d], Steffen Bugge [a], Geir Bjørkøy [c,d], Eirik Sundby [b], Bård Helge Hoff [a,*]

[a] Norwegian University of Science and Technology, Department of Chemistry, Høgskoleringen 5, NO-7491 Trondheim, Norway
[b] Sør-Trøndelag University College, E.C. Dahls gt. 2, NO-7004 Trondheim, Norway
[c] Norwegian University of Science and Technology, Department of Cancer Research and Molecular Medicine, Prinsesse Kristinas gt. 1, NO-7006 Trondheim, Norway
[d] Sør-Trøndelag University College, Erling Skjalgssons gt. 1, NO-7004 Trondheim, Norway

ARTICLE INFO

Article history:
Received 24 February 2014
Received in revised form 11 April 2014
Accepted 16 April 2014
Available online xxxx

Keywords:
Pyrrolopyrimidine
Tyrosine kinase
EGFR-TK
Src-kinase
Cancer
CSF1R kinase
Erlotinib
Druglike properties

Chemical compounds studied in this article:
Benzylamine (PubChem CID: 7504)
1-Phenylethanamin (PubChem CID: 7408)
PKI-166 (PubChem CID: 6918403)
2-Amino-2-phenylethan-1-ol (PubChem CID: 92466)
2-Methoxyphenylboronic acid (PubChem CID: 2733958)
4-(Hydroxymethyl)phenylboronic acid (PubChem CID: 2734706)
PKI-166 (PubChem CID: 6918403)
Erlotinib (PubChem CID: 176870)

ABSTRACT

The epidermal growth factor receptor is an important target in molecular cancer therapy. Herein, the enzymatic inhibition potential of a series of chiral and non chiral pyrrolopyrimidine based derivatives have been investigated and optimised. Overall, seven new compounds were identified having enzymatic IC_{50} values comparable to or better than the commercial drug Erlotinib. High activity was also confirmed towards the epidermal growth factor receptor L858R and L861Q mutants. Based on calculated druglike properties, eight compounds were further evaluated towards a panel of 52 other kinases revealing interesting Src-family kinase and colony stimulating factor 1 receptor kinase inhibitory activity. Cell proliferation studies with the cell lines A431, C-33A, AU-565, K-562 and genetically engineered Ba/F3-EGFR^{L858R} cells also showed several molecules to be more active than Erlotinib, and thus confirming these pyrrolopyrimidines as attractive drug candidates or lead structures.

1. Introduction

The epidermal growth factor receptor (EGFR/HER1) and other human epidermal growth factor receptors (HER's) are often amplified, overexpressed or mutated in solid tumours (Hynes and MacDonald, 2009; Soonthornthum et al., 2011; Sun et al., 2012; Yarden and Pines, 2012). Auto phosphorylation of tyrosine residues on these HER's provide docking sites for mediators of downstream

* Corresponding author. Tel.: +47 73593973; fax: +47 73594256.
E-mail addresses: Svein.jacob.kaspersen@chem.ntnu.no (S.J. Kaspersen), Jin.han@chem.ntnu.no (J. Han), kristin.norsett@ntnu.no (K.G. Nørsett), line.rydsa@sintef.no (L. Rydså), eli.kjobli@hist.no (E. Kjøbli), steffen.bugge@chem.ntnu.no (S. Bugge), geir.bjorkoy@hist.no (G. Bjørkøy), E.Sundby@hist.no (E. Sundby), bard.helge.hoff@chem.ntnu.no (B.H. Hoff).
[1] Present address: SINTEF Energy Research, Postbox 4761 Sluppen, NO-7465 Trondheim, Norway.

http://dx.doi.org/10.1016/j.ejps.2014.04.011
0928-0987/

signalling eventually leading to cellular proliferation, migration, differentiation and survival. EGFR is mainly localised at the plasma membrane, but is also present in cellular organelles, the nucleus and mitochondria (Irwin et al., 2011).

The HER members can be inhibited with small molecules or monoclonal antibodies (Nedergaard et al., 2012). Due to the heterogeneity of various tumours, the usefulness of these strategies depends on the oncogenic profile of the cancer. As single agents epidermal growth factor receptor tyrosine kinase (EGFR-TK) inhibitors as Erlotinib and Gefitinib have been found most effective in non-small cell lung cancer leading to increased progression free survival in specific patient groups (Koehler and Schuler, 2013; Sgambato et al., 2012). Erlotinib and Gefitinib, which both have activity towards wild-type EGFR and the $EGFR^{L858R}$ mutant, are now approved for 1st line therapy in the clinic (Sgambato et al., 2012). Interestingly, it has been shown that Erlotinib bind both to the active and inactive form of EGFR (Park et al., 2012). When targeting HER receptor kinases in a therapeutic setting, a high overall HER inhibitory activity is likely to improve efficiency, as there is a considerable activation by heterodimerisation and cross-talk between the HER members (Tebbutt et al., 2013). Although both HER3 and HER4 might be of importance, the HER2 receptor has been most intensively studied. Inhibitors like Lapatinib have been found efficient in HER2 positive breast cancer.

While these reversible ATP competitive inhibitors have some adverse effects (Sugiura et al., 2013; Yoshida et al., 2013), the major drawback is that resistance is often emerging, either by a second mutation ($EGFR^{T790M}$) or by up-regulating of alternative signalling pathways (Chong and Jaenne, 2013). The $EGFR^{T790M}$ mutant can be targeted using irreversible inhibitors. Although these agents hold much promise (Carmi et al., 2012), they have a challenging toxicity profile not seen for the reversible inhibitors (Barf and Kaptein, 2012). Thus, the clinical benefit therefore still seems somewhat limited (Sequist et al., 2010; Landi and Cappuzzo, 2013).

If however, the cancer therapy is based on hitting two or more targets, there is a lower risk of resistance development. The established reversible type inhibitors are therefore investigated in combination with other kinase inhibitors, chemical agents, monoclonal antibodies and radiotherapy (Tebbutt et al., 2013; Wu et al., 2013; Lainey et al., 2013). Alternatively, inhibitors can be developed to possess activity towards more than one kinase. Among others, the Src-family of kinases has been identified as viable targets (Lu et al., 2012; Kim et al., 2009). Src's are known to interact both with EGFR and HER2, but also other kinases and signal transduction systems and mitochondrial functions (Irwin et al., 2011; Kim et al., 2009; Hebert-Chatelain, 2013). Examples of Src inhibitors include Dasatinib, Bosutinib and Saracatinib, Fig. 1.

Previously known pyrrolopyrimidine based EGFR-TK inhibitors include PKI-166 (Traxler, 2003) and AEE-788 (Traxler et al., 2004; Park et al., 2005). Our laboratory has recently developed highly active thienopyrimidine based EGFR-TK inhibitors (Structure **I**, Fig. 1) (Bugge et al., 2014). However, based on our earlier investigation on pyrrolopyrimidines (Kaspersen et al., 2011), we envisioned that even more potent inhibitors with better druglike properties could be obtained by applying design principals revealed in the thienopyrimidine study (Bugge et al., 2014).

Establishment of a new synthetic route, allowed for a more elaborate investigation of substituent effects in the 6-aryl group of the 7*H*-pyrrolo[2,3-*d*]pyrimidine scaffold. Thus, by a SAR study and a step-wise combination of favourable substitution patterns, several highly potent pyrrolopyrimidine based EGFR-TK inhibitors were identified. These derivatives also possess interesting inhibitory effects on Src-family of kinases, HER2, HER4 and colony stimulating factor 1 receptor kinase (CSF1R). Moreover, the new compounds also possess promising activity as compared to Erlotinib in genetically engineered Ba/F3-$EGFR^{L858R}$ cells and in human cancer cell lines.

2. Material and methods

2.1. Chemicals

Compounds (*R*)-1-phenylethanamine ((*R*)-**2**), (*R*)-1-(2-chlorophenyl)ethan-1-amine ((*R*)-**4**), (*R*)-1-(2-methoxyphenyl)ethan-1-amine ((*R*)-**6**), (*R*)-2-(1-aminoethyl)phenol ((*R*)-**7**), 4-nitro-1-phenylethan-1-amine ((*R*)-**13**), benzylamine (**17**), (*R*)-1-(phenyl)-1-propanamine ((*R*)-**21**), (*R*)-2-methoxy-1-phenylethan-1-amine ((*R*)-**25**), (*S*)-2-amino-2-phenylethan-1-ol ((*S*)-**24**), 1-4-(*tert*-butyl)phenyl)ethanone, sodium *tert*-butoxide, 2,2-dimethyl-1-phenylpropan-1-one, sodium borohydride, sodium cyanoborohydride, iodomethane (2 M in *tert*-butyl methyl ether), palladium(II) acetate, 2-dicyclohexylphosphino-2′,4′,6′-triisopropylbiphenyl (XPhos), chloro(2-dicyclohexylphosphino-2′,4′,6′-triisopropyl-1,1′-biphenyl)[2-(2′-amino-1,1′-biphenyl)]palladium(II) (XPhos Pd G2), boron tribromide were from Sigma–Aldrich. (4-Formyl-2-methoxyphenyl)boronic acid was from Combi-Blocks, while the other arylboronic acids were from Sigma–Aldrich. (*R*)-2-Methyl-1-phenylpropan-1-amine ((*R*)-**22**) was from ABCR, (*S*)-2-amino-2-(4-fluorophenyl)acetic acid was from Fluorochem, and compound **50** was from Nanjing Pharmatechs. Compound **1a**–**1d** were prepared as described previously (Kaspersen et al., 2011). Silica-gel column chromatography was performed using silica gel 60 Å from Fluka, pore size 40–63 μm. Celite 545 from Fluka was also used.

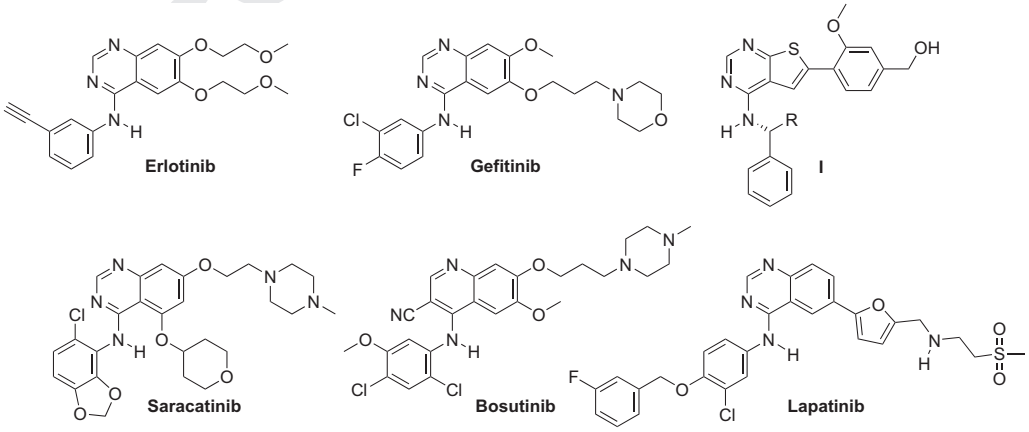

Fig. 1. Examples of reversible EGFR-TK, HER2 and dual ABL/Src kinase inhibitors.

Please cite this article in press as: Kaspersen, S.J., et al. Identification of new 4-*N*-substituted 6-aryl-7*H*-pyrrolo[2,3-*d*] pyrimidine-4-amines as highly potent EGFR-TK inhibitors with Src-family activity. Eur. J. Pharm. Sci. (2014), http://dx.doi.org/10.1016/j.ejps.2014.04.011

2.2. Analyses

^{1}H and ^{13}C NMR spectra were recorded with Bruker Avance 400 spectrometer operating at 400 MHz and 100 MHz, respectively. ^{19}F NMR was performed on a Bruker Avance 500 operating at 564 MHz. For ^{1}H and ^{13}C NMR chemical shifts are in ppm rel. to TMS or DMSO-d_6, while for ^{19}F NMR the shift values are relative to hexafluorobenzene. Coupling constants are in hertz. HPLC (Agilent 110-Series) with a G1379A degasser, G1311A Quatpump, G1313A ALS autosampler and a G1315D Agilent detector (230 nm) was used to determine the purity of the synthesised compounds. All compounds evaluated for EGFR inhibitory potency had a purity of ⩾95%. Conditions: Poroshell C18 (100 × 4.6 mm) column, flow rate 0.8 ml/min, elution starting with water/acetonitrile (90/10), 5 min isocratic elution, then linear gradient elution for 35 min ending at acetononitrile/water (100/0). The software used with the HPLC was Agilent ChemStation. Accurate mass determination (ESI) was performed on an Agilent G1969 TOF MS instrument equipped with a dual electrospray ion source, or EI (70 eV) using a Finnigan MAT 95 XL. Accurate mass determination in positive and negative mode was performed on a "Synapt G2-S" Q-TOF instrument from Waters. Samples were ionized by atmospheric-pressure chemical ionization (ACPI) and analysed using an atmospheric solids analysis probe (ASAP). No chromatography separation was used before the mass analysis. FTIR spectra were recorded on a Thermo Nicolet Avatar 330 infrared spectrophotometer. All melting points are uncorrected and measured by a Stuart automatic melting point SMP40 apparatus.

2.3. General synthetic procedures

2.3.1. Thermal amination of 4-chloro-pyrrolo[2,3-d]pyrimidines

Compound **1a–d** or **54** (1 mmol) was mixed with the selected amine, **2–25**, (3 mmol) and *n*-butanol (5 ml) and agitated at 145 °C for 14–24 h. Then the mixture was cooled to 22 °C, diluted with water (15 ml) and ethyl acetate (40 ml). After phase separation, the water phase was back extracted with more ethyl acetate (2 × 10 ml). The combined organic phases were washed with brine (10 ml), dried over anhydrous Na_2SO_4, filtered and concentrated *in vacuo*, before the crude mixture was purified as specified for each individual compound.

2.3.2. Suzuki coupling on 6-iodopyrrolo[2,3-d]pyrimidines

The following is representative: Compound (*R*)-**56** (300 mg, 0.825 mmol) was mixed with (2-methoxyphenyl)boronic acid (150 mg, 0.989 mmol), fine powdered K_2CO_3 (398 mg, 2.88 mmol), XPhos (20 mg, 0.040 mmol), 2nd generation XPhos precatalyst (34 mg, 0.04 mmol), 1,4-dioxane (2 ml) and water (2 ml). The reaction was then stirred at 100 °C for 1.5–18 h under nitrogen atmosphere. The solvent was removed and the product was diluted with water (20 ml) and extracted with ethyl acetate (30 ml). The water phase was extracted with more ethyl acetate (3 × 30 ml). The combined organic phases were washed with brine (20 ml), dried over anhydrous Na_2SO_4, filtered and concentrated *in vacuo*. The crude mixture was purified as specified for each individual compound. The synthesis and spectroscopic data of all new compounds are given in the Supporting information.

2.4. Biochemical profiling of kinase inhibitors

2.4.1. In vitro EGFR (ErbB1) and EGFR mutant inhibitory potency

The compounds were supplied in a 10 mM DMSO solution, and enzymatic EGFR (ErbB1) inhibition potency was determined by Invitrogen (LifeTechnology) using their Z'-LYTE® assay technology (Pollok et al., 2000). All compounds were first tested for their inhibitory activity at 100 nM in duplicates. The potency observed at 100 nM was used to set starting point of the IC_{50} titration curve, in which three levels were used 100, 1000 or 10,000 nM. The IC_{50} values reported are based on the average of at least 2 titration curves (minimum 20 data points), and were calculated from activity data with a four parameter logistic model using SigmaPlot (Windows Version 12.0 from Systat Software, Inc.). Unless stated otherwise the ATP concentration used was equal to K_m. The average standard deviation for single point measurements were <4%. The inhibitory potency towards EGFR mutants was determined in the same way.

2.4.2. Ba/F3 cell reporter cell analysis

Transfected Ba/F3 cells containing expression vectors for the L858R and T790M EGFR mutants were a kind gift from Dr. Nikolas von Bubnoff at the Technical University of Munich, Munich, Germany (Kancha et al., 2009). The cells were cultured in RPMI 1640 (Gibco, Invitrogen) supplemented with 10% FCS (Gibco, Invitrogen), 1% L-glutamine (Gibco, Invitrogen) and 0.1% Gentamycin (Sanofi Aventis). Erlotinib was purchased from LC Laboratories (Woburn, MA). All inhibitors were reconstituted in DMSO, and appropriate stock solutions were prepared using cell culture medium. The final percentage concentrations of DMSO were <0.2%. Proliferation analysis: Ba/F3 cells (1×10^4 per well) were plated into 96-well plates. Inhibitors were added in different concentrations as indicated. Cell growth was measured at 48 h using TACS® XTT Cell Proliferation Assay (Trevigen) according to the manufacturer's instructions.

2.4.3. Human cancer cell lines A-431 and K-562

Cell proliferation assays were performed by ReactionBiology Corp. A-431 human epidermal carcinoma and K-562 chronic myelogenous leukaemia cell lines were obtained from American Type Culture Collection (Manassas, VA). Staurosporine was obtained from Sigma–Aldrich (Saint Louis, MI). Cell Titer-Glo® Luminescent cell viability assay reagent was obtained from Promega (Madison, WI). A-431 and K-562 cells were grown in Dulbecco's Modified Eagle Medium (DMEM). Both cell culture mediums were supplemented with 10% heat-inactivated fetal bovine serum (FBS), 100 μg/ml penicillin, and 100 μg/ml of Streptomycin. Cultures were maintained at 37 °C in a humidified atmosphere of 5% CO_2 and 95% air. Compound (*R*)-**26l**, (*R*)-**26n**, **41n**, (*S*)-**48b**, (*S*)-**48e**, (*S*)-**48l**, (*S*)-**48n**, (*S*)-**60n**, Erlotinib and Staurosporine (positive control) were all dissolved in DMSO in 10 mM stock. Culture medium (10 μl) was added to each well of 384 well cell culture plates. The compounds were diluted in a source plate in DMSO at 3-fold serial dilutions starting at 10 mM, total 10 doses. The compounds (0.25 μl) were delivered from source plate to each well of the cell culture plates by Echo 550. Then, 15 μl of culture medium containing 5000 cells of A-431 or K-562 were added to the wells of the cell culture plates. The cells were incubated with the compounds at 37 °C, 5% CO_2 for 72 h. 25 μl of Cell Titer Glo reagent (25 μl) was added to each well according to the instruction of the kit. The contents were mixed on an orbital shaker for 2 min and incubated at room temperature for 10 min to stabilize luminescent signal. Luminescence was recorded by Envision 2104 Multilabel Reader (PerkinElmer, Santa Clara, CA). The maximum luminescence for each cell line in the absence of test compound, but in the presence of 0.4% DMSO, was similarly recorded after incubation for 72 h. The number of viable cells in the culture was determined based on quantitation of the ATP present in each culture well. The percentage growth after 72 h (*%-growth*) was calculated as follows: 100% × (*luminescence t* = 72 h/*luminescence* untreated, *t* = 72 h).

2.4.4. Human cancer cell line testing AU-565 and C-33A

Cell proliferation assays were performed by Netherlands Translational Research Center B.V (NTRC). All cell lines were licensed

from the American Type Culture Collection (ATCC) Manassas, Virginia (US). Master and working cell banks (MCB and WCB) were prepared by subculturing in ATCC-recommended media and freezing according to ATCC recommended protocols (www.atcc.org). Cell line stocks for the assays were prepared from the WCB. The MCB, WCBs and assay stocks were prepared within respectively 3, 6 and 9 passages of the ATCC vial. Proliferation analysis: Compounds were weighed on a calibrated balance and dissolved in 100% DMSO to a concentration of 10 mM. The samples were stored at room temperature. The compound stock was diluted in 3.16-fold steps in 100% DMSO to obtain a 10-point dilution series. This was further diluted 31.6 times in 20 mM sterile Hepes buffer pH 7.4. A volume of 5 ml was transferred to the cells to generate a test concentration range from 3.16×10^{-5} M to 3.16×10^{-9} M in duplicate. The final DMSO concentration during incubation was 0.4% in all wells. An assay stock was thawed and diluted in its ATCC recommended medium and dispensed in a 384-well plate, depending on the cell line used, at a concentration of 400–1600 cells per well in 45 μl medium. For each used cell line the optimal cell density was used. The margins of the plate were filled with phosphate-buffered saline. Plated cells were incubated in a humidified atmosphere of 5% CO_2 at 37 °C. After 24 h, 5 μl of compound dilution was added and plates were further incubated for another 72 h. After 72 h, 25 μl of ATPlite 1Step™ (PerkinElmer) solution was added to each well, and subsequently shaken for 2 min. After 10 min of incubation in the dark, the luminescence was recorded on an Envision multimode reader (PerkinElmer). The maximum luminescence for each cell line in the absence of test compound, but in the presence of 0.4% DMSO, was similarly recorded after incubation for 72 h (*luminescence* untreated, $t = 72$ h). The percentage growth after 72 h (*%-growth*) was calculated as follows: 100% × (*luminescence* $t = 72$ h/*luminescence* untreated, $t = 72$ h). IC_{50} values were calculated from % growth and compound concentration with a four parameter logistic model using SigmaPlot (Windows Version 12.0 from Systat Software, Inc.).

Controls: $t = 0$ h signal: On a parallel plate, 45 μl cells were dispensed and incubated in a humidified atmosphere of 5% CO_2 at 37 °C. After 24 h 5 μl DMSO-containing Hepes buffer and 25 μl ATPlite 1Step™ solution were mixed, and luminescence measured after 10 min incubation (=*luminescence*, $t = 0$ h). Positive control: The IC_{50} of the reference compound doxorubicin was measured on a separate plate. The IC_{50} was trended. If the IC_{50} is out of specification (0.32–3.16 times deviating from historic average) the assay is invalidated. Cell growth control: The cellular doubling times of all cell lines were calculated from the $t = 0$ h and $t = 72$ h growth signals of the untreated cells. If the doubling time is out of specification (0.5–2.0 times deviating from historic average) the assay is invalidated.

2.5. Molecular modelling and calculations

2.5.1. Molecular modelling

The X-ray crystal structures of the protein 2J6M (Wild-type EGFR) and protein 2IJU ($EGFR^{T790M}$) were prepared using the protein preparation wizard, which is part of the Maestro software package (Maestro, v8.5; Schrödinger, LLC, New York, NY, USA). Bond orders and formal charges were added for het-groups, and hydrogens were added to all atoms in the system. Water molecules beyond 5 Å from het-groups were removed. To alleviate steric clashes that may exist in the original PDB structures, an all-atom constrained minimization was carried out with the Impact Refinement module (Impref) (Impact, v5.0; Schrödinger, LLC) using the OPLS-2005 force field. The minimization was terminated when the energy converged or the RMSD reached a maximum cutoff of 0.30 Å. The resulting protein structures were used in the following docking study. Ligands were drawn using ChemBioDraw (ChemBioDraw Ultra 13.0, CambridgeSoft, PerkinElmer) and were prepared using LigPrep2.2 (LigPrep, v2.2; Schrödinger, LLC). For the computational investigation of the receptor-inhibitor structures, the energy minimized structures of 2J6M and ligands were subsequently docked using induced-fit docking (IFD) of Schrödinger (Sherman et al., 2006a,b; Fit Docking Protocol, 2013). The resulting docked poses were analyzed using Glide pose viewer tool. All the graphical pictures were made using Maestro.

2.5.2. Calculated druglike properties

The relative druglike properties of compounds were calculated from IC_{50} values (pIC_{50}). Note that the obtained values are assay dependant and therefore less valid when comparing studies using other assay formats. Equations used for LE, BEI, and SEI calculations can be found in Meanwell (2011), while LELP = log *P*/LE was from Keserue and Makara (2009). The number of heavy atoms used in calculation of LE includes all non-hydrogen atoms, and for BEI calculation the molecular weight used is in kDa. The values for polar surface area used in calculation of SEI were estimated as described by Ertl et al. (2000). (Online resource: http://www.daylight.com/meetings/emug00/Ertl/tpsa.html). The calculated log *P* (clog *P*) was determined with OSIRIS Property Explorer: http://www.organic-chemistry.org/prog/peo/.

2.5.3. Gini calculations

Quantification of compounds kinase selectivity by the use of Gini plots and Gini coefficients followed the procedure previously reported (Graczyk, 2007).

3. Result and discussion

3.1. Design of the inhibitors

Pyrrolopyrimidines have previously been investigated as EGFR-TK inhibitors by us and others (Traxler et al., 2004; Kaspersen et al., 2011; Caravatti, 2004; Grotzfeld et al., 2005). However, in the case of 4-*N*-substituted 6-aryl-7*H*-pyrrolo[2,3-*d*]pyrimidine-4-amines, detailed knowledge of the effect of substitution in the 6-aryl and the 4-amino group is limited. Moreover, our previous study on thienopyrimidines as EGFR-TK inhibitors (Bugge et al., 2014) showed both that the activity could be increased by proper substitution of these groups, but also that the pyrrolopyrimidines had an intrinsic higher potency than the corresponding thienopyrimidines. Thus, it was apparent that the full potential of the pyrrolopyrimidine scaffold was not yet realised.

As our aim was to use structure–activity relationships to identify highly potent inhibitors, we investigated effects of variations

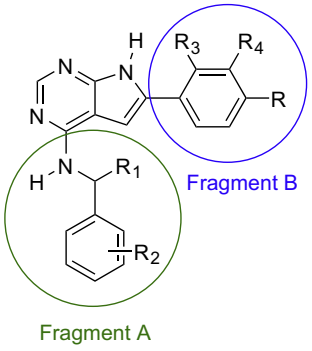

Fig. 2. The study of pyrrolopyrimidine based EGFR-TK inhibitors was performed by structural variations in the 4-amino-(Fragment A) and the 6-aryl (Fragment B) groups.

Please cite this article in press as: Kaspersen, S.J., et al. Identification of new 4-*N*-substituted 6-aryl-7*H*-pyrrolo[2,3-*d*] pyrimidine-4-amines as highly potent EGFR-TK inhibitors with Src-family activity. Eur. J. Pharm. Sci. (2014), http://dx.doi.org/10.1016/j.ejps.2014.04.011

of the pyrrolopyrimidine in both the 4-benzylamine part (Fragment A) and the 6-aryl part (Fragment B), Fig. 2.

In Fragment A, the R_1-substituent was modified in terms of bulk size, and also by introducing hydrogen bond accepting and donating groups. In the aromatic part of Fragment A, our previous study indicated size limitations in this part of the binding pocket (Kaspersen et al., 2011). Herein, this is explored in more detail. In addition fluorinated derivatives were included due to their general positive effect on metabolic stability (Böhm et al., 2004; Wu et al., 2003). The investigation of structural variations in Fragment B on EGFR-TK potency was inspired by our recent discoveries of active thienopyrimidine based inhibitors (structure **I**, Fig. 1) (Bugge et al., 2014).

3.2. Synthesis

To enable efficient synthesis of a compound library, two different, but complementary routes were used. Compounds with structural variation in the 4-position (Fragment A) were derived by a method starting from 1-aryl-2-bromoethanones giving in three steps the 6-aryl-4-chloropyrrolopyrimidines **1a–d** (Kaspersen et al., 2011, 2012). Amination chemistry in *n*-butanol gave the 4,6-disubstituted pyrrolopyrimidines **26–49**, with varying R, R_1 and R_2 substituents as shown in Scheme 1. Derivatives **26–47** were in most cases prepared as their pure (*R*)-enantiomer, except **29a**, **33a**, **39a**, **40a**, **47b** which were racemates, (*S*)-**26a** included as a model to test for effect of stereochemistry, and (*S*)-**48b–d** and (*S*)-**49b** in which the stereochemical nomenclature changes as a result of the higher priority of the CH_2—O group as compared to the aromatic ring.

Whereas the initial strategy might be highly useful in a production setting, it was not suited for generating a larger library of derivatives with variations in the 6-aryl group (Fragment B). Therefore, an alternative route was established, using Suzuki coupling to incorporate the targeted structural variations, see Scheme 2.

First, the commercially available compound **50** was converted to **52** by standard chlorination and protection. The following iodination has previously been performed by others (Engelhardt et al., 2010), but preparative HPLC was needed to purify the iodo compound **53**. The initial 100–500 mg scale reaction resulted in sub-optimal conversion and formation of an unidentified by-product. However, the chemistry improved on scaling to gram scale. Finally the reaction was performed in a 10 gram scale. By crystallisation from acetonitrile compound **53** could be isolated in 74% yield and 99% purity.

Amination of **53** was attempted using (*R*)-1-phenylethanamine (**2**), but gave a mixture of the protected and unprotected analogues. Instead, the pyrrolopyrimidine **54** obtained by deprotection, could be transformed to give the precursors **56–59** in 56–86% non-optimised yield. Suzuki coupling at C-6 using XPhos and 2nd generation XPhos precatalyst (Kinzel et al., 2010) was then performed using selected arylboronic acids giving most of the targeted products. However, applying *ortho*- and *meta*-hydroxyphenylboronic acids, the coupling only reached 50% conversion in 40 h. Instead, these derivatives were made by deprotection of the methoxy analogues (*R*)-**26e** and (*R*)-**26g**. The *para*-hydroxymethyl derivatives (*R*)-**26n**, **41n**, (*S*)-**48n** and (*S*)-**60n** were obtained by sodium borohydride reduction of the corresponding aldehyde derivatives (*R*)-**26m**, **41m**, (*S*)-**48m** and (*S*)-**60m**.

3.3. In vitro enzymatic inhibition study

3.3.1. Structural variation in the benzylamine part (Fragment A)

The effect of structural variations in Fragment A on EGFR-TK potency was initially studied with *para*-methoxyphenyl as the C-6 substituent and 21 structural variations in Fragment A. The EGFR-TK enzymatic potency was determined by single point measurements in duplicates at 100 nM test concentration. This was followed by IC_{50} 10-point titration measurements also in duplicate. Erlotinib in the same assay had an EGFR-TK inhibitory potency of 0.4 nM. Fig. 3 highlights the most important findings with respect to the tolerated aromatic substitution pattern in Fragment A. High EGFR-TK potency was achieved for compounds based on (*R*)-1-phenylethanamine, (*R*)-**26a**, benzylamine, **41a**, and (*R*)-l-phenylpropylamine, (*R*)-**45a**. In case of compound **26a** the (*R*)-enantiomer was approximately 16 times more active than (*S*)-**26a**. All compounds containing fluoro substituents maintained a high potency. The *ortho* and *meta* methyl derivatives (*rac*)-**29a** and (*rac*)-**33a** also showed promising activity. Due to the low IC_{50} values seen for the *ortho* fluorinated analogue (*R*)-**27a** and the *ortho*-methyl substituted (*rac*)-**29a**, we also prepared and tested the *ortho*-chloro, (*R*)-**28a**, -hydroxyl, (*R*)-**31a**, and the -methoxy, (*R*)-**30a**, analogues. Whereas the former two had potency of 8.1 and 6.6 nM respectively, the methoxy derivative was considerable less active (IC_{50} = 105 nM).

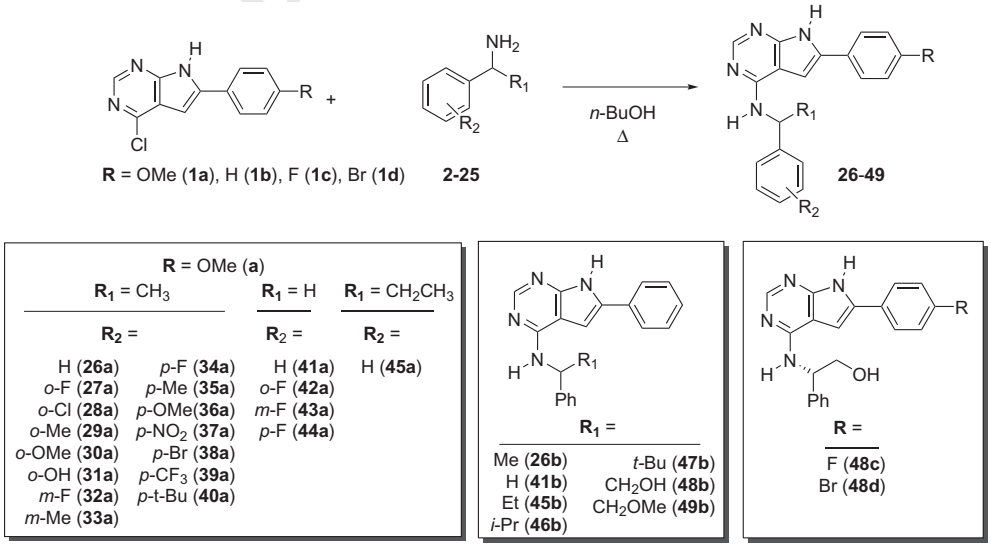

Scheme 1. Synthetic route for preparation of the pyrrolopyrimidine derivatives **26–49**.

Please cite this article in press as: Kaspersen, S.J., et al. Identification of new 4-*N*-substituted 6-aryl-7*H*-pyrrolo[2,3-*d*] pyrimidine-4-amines as highly potent EGFR-TK inhibitors with Src-family activity. Eur. J. Pharm. Sci. (2014), http://dx.doi.org/10.1016/j.ejps.2014.04.011

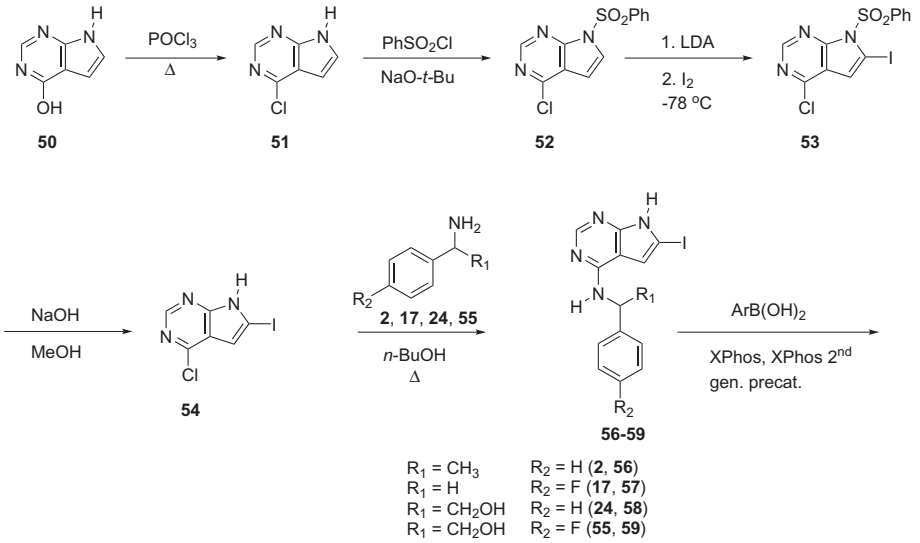

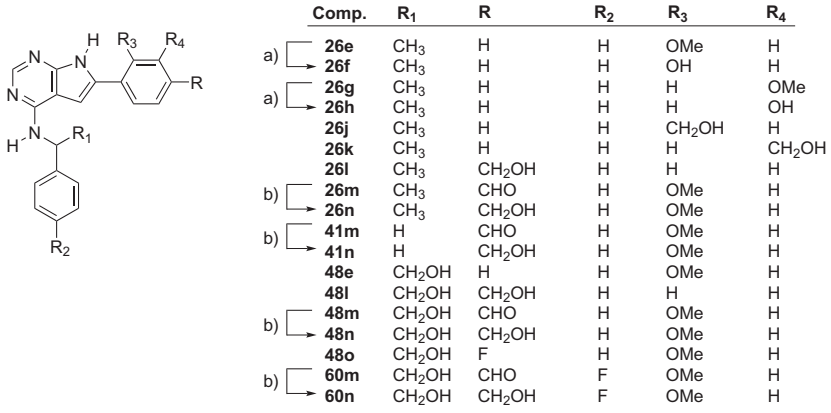

	Comp.	R_1	R	R_2	R_3	R_4
a)	**26e**	CH_3	H	H	OMe	H
	26f	CH_3	H	H	OH	H
a)	**26g**	CH_3	H	H	H	OMe
	26h	CH_3	H	H	H	OH
	26j	CH_3	H	H	CH_2OH	H
	26k	CH_3	H	H	H	CH_2OH
	26l	CH_3	CH_2OH	H	H	H
b)	**26m**	CH_3	CHO	H	OMe	H
	26n	CH_3	CH_2OH	H	OMe	H
b)	**41m**	H	CHO	H	OMe	H
	41n	H	CH_2OH	H	OMe	H
	48e	CH_2OH	H	H	OMe	H
	48l	CH_2OH	CH_2OH	H	H	H
b)	**48m**	CH_2OH	CHO	H	OMe	H
	48n	CH_2OH	CH_2OH	H	OMe	H
	48o	CH_2OH	F	H	OMe	H
b)	**60m**	CH_2OH	CHO	F	OMe	H
	60n	CH_2OH	CH_2OH	F	OMe	H

Scheme 2. Pyrrolopyrimidines synthesized by Suzuki coupling on **56**–**59** giving (*R*)-**26e**–**h**, (*R*)-**26j**–**n**, **41m**–**n**, (*S*)-**48e**, (*S*)-**48l**–**n** and (*S*)-**60m**–**n**. (a) BBr_3 and (b) $NaBH_4$ in MeOH.

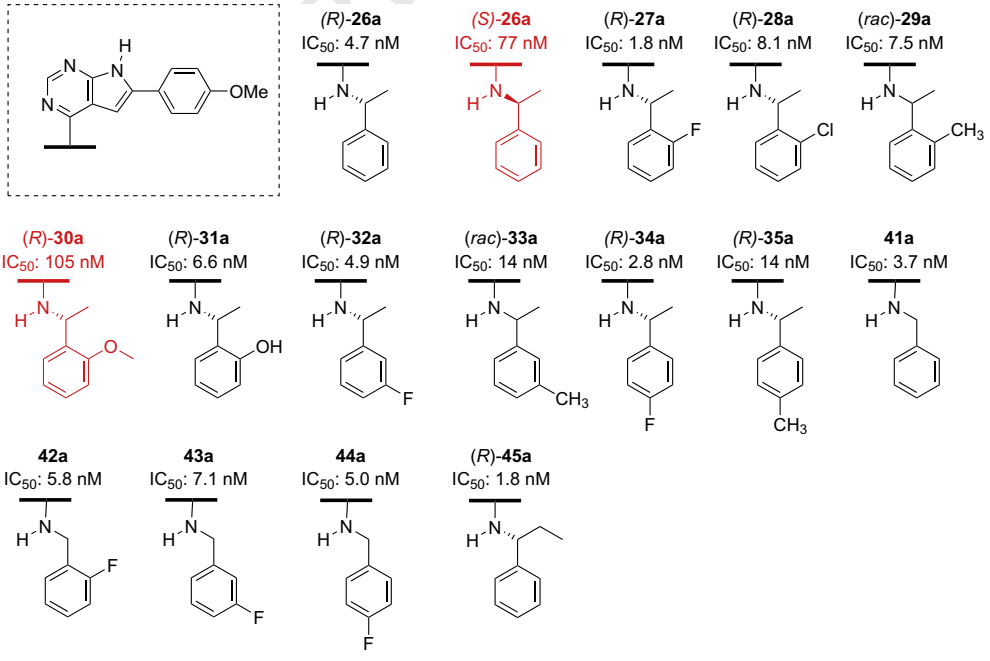

Fig. 3. EGFR-TK enzymatic IC_{50} values (nM) for selected substitution patterns. See Supporting information for single point data and standard deviations.

Please cite this article in press as: Kaspersen, S.J., et al. Identification of new 4-*N*-substituted 6-aryl-7*H*-pyrrolo[2,3-*d*] pyrimidine-4-amines as highly potent EGFR-TK inhibitors with Src-family activity. Eur. J. Pharm. Sci. (2014), http://dx.doi.org/10.1016/j.ejps.2014.04.011

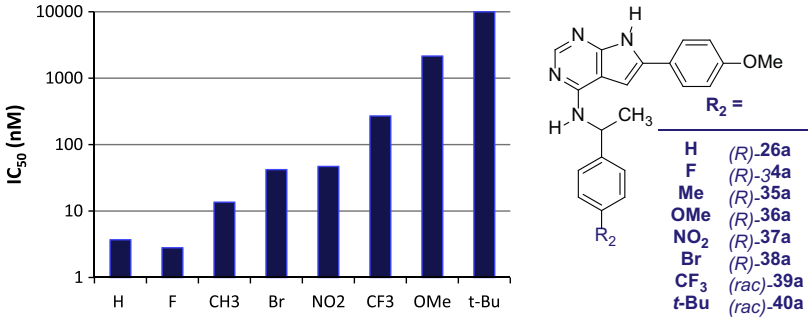

Fig. 4. Effect of *para* substitution on EGFR-TK IC_{50} values (nM). IC_{50} values are presented in log scale. See Supporting information for single point data and standard deviations.

Five more *para* substituted derivatives (Br, NO_2, OMe, CF_3, *t*-Bu) were assayed giving IC_{50} values ranging from 40 to >10,000 nM, see Fig. 4. Inspection of these data suggests that the activity is reduced with increase in bulk size. However, as the trifluoromethyl substituted compound was more active than the *para*-methoxy analogue, the electronic content of the aromatic ring might also be of importance.

Based on the excellent IC_{50} value of the ethyl derivative (*R*)-**45a**, and previous discoveries on thienopyrimidines (Bugge et al., 2014) and furopyrimidines (Peng et al., 2013), it was also decided to investigate the effect of the alkylamine side chain on EGFR-TK activity. In this study the 6-position of the pyrrolopyrimidine was substituted with a phenyl ring. As seen from Table 1, the activity was not dramatically affected by the steric bulk of the R_1-substituent.

Moreover, insertion of the CH_2OH group in compound (*S*)-**48b** improved the IC_{50} value down to 0.7 nM. The effect seen was similar to that observed in thienopyrimidine analogues (Bugge et al., 2014), and modelling using an induced fit procedure (Sherman et al., 2006a,b), explains this by hydrogen bonding to the DFG motif as seen in Fig. 5.

As the presence of the hydroxymethyl group also increases the weight and the hydrophilicity of the compounds, the relative drug-like properties of the candidate inhibitors were evaluated using metrics as ligand efficiency (LE), binding efficiency (BEI), surface efficiency index (SEI), and ligand-efficiency-dependent lipophilicity (LELP) (Keserue and Makara, 2009; Hopkins et al., 2004; Abad-Zapatero and Metz, 2005; Abad-Zapatero, 2007; Leeson and Springthorpe, 2007). The LE values of the various compounds are shown in Fig. 6, while BEI, SEI and LELP are given in Fig. 7. LE and BEI are measures of binding efficiency per heavy atom and molecular weight, respectively, and the higher the better. In terms of LE and BEI the hydroxymethyl compound (*S*)-**48b**, the methyl analogue (*R*)-**26b** and the benzylamine based **41b** were concluded most promising.

Too high polarity might lead to poor membrane permeability. SEI describes how dependent activity is of polar interactions. Erlotinib and (*S*)-**48b** were found to have comparable SEI values, while the others are less polar. On the other hand, drug candidates being too lipophilic will have poor solubility and higher risk of failure due to toxic effects (Meanwell, 2011). LELP is used to assess

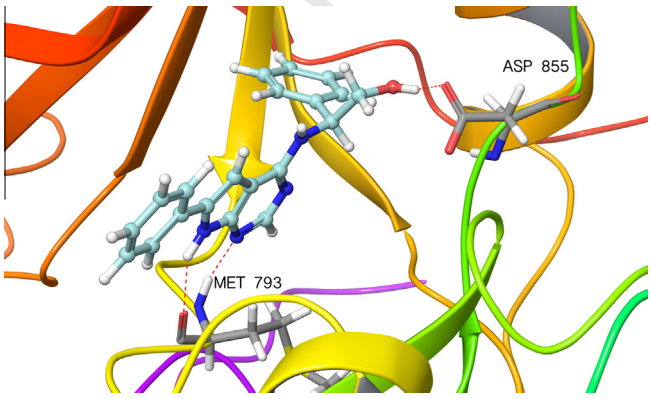

Fig. 5. Binding of compound (*S*)-**48b** to the EGFR-TK ATP binding site based on the crystal structure 2J6M (Yun et al., 2007). The compound is indicated to engage in hydrogen bonding via the hydroxymethyl group to Asp855 in the DFG motif, by N-1 to back-bond NH of Met793 and by the pyrrolo nitrogen to the carbonyl oxygen of Met793.

Table 1
EGFR-TK inhibitory potency given as % inhibition at 100 nM and IC_{50} values (nM) upon variation of the R_1 substituent. Unless otherwise noted IC_{50} values are based on duplicate measurements.

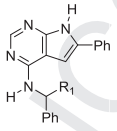

Entry	Compound	R_1	EGFR inhibition (%)	IC_{50} (nM)
1	(*R*)-**26b**	CH_3	95	3.2 ± 0.6[a,b]
2	**41b**	H	97	3.8 ± 1.1
3	(*R*)-**45b**	CH_2CH_3	91	5.4 ± 1.5
4	(*R*)-**46b**	$CH(CH_3)_2$	84	15 ± 1
5	(*rac*)-**47b**	$C(CH_3)_3$	88	10 ± 3
6	(*S*)-**48b**	CH_2OH	98	0.7 ± 0.3[b]
7	(*S*)-**49b**	CH_2OMe	100	1.8 ± 0.1
8	**Erlotinib**	[c]	100	0.4 ± 0.1[d]

[a] Previously known EGFR-TK inhibitor, Kaspersen et al. (2011).
[b] Four IC_{50} titrations (40 data points).
[c] For structure see Fig. 1.
[d] Six IC_{50} titrations (60 data points).

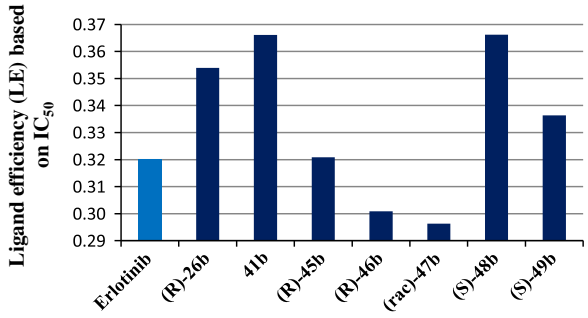

Fig. 6. Ligand efficiency (LE) for Erlotinib and pyrrolopyrimidines having variable R_1-groups.

Please cite this article in press as: Kaspersen, S.J., et al. Identification of new 4-*N*-substituted 6-aryl-7*H*-pyrrolo[2,3-*d*] pyrimidine-4-amines as highly potent EGFR-TK inhibitors with Src-family activity. Eur. J. Pharm. Sci. (2014), http://dx.doi.org/10.1016/j.ejps.2014.04.011

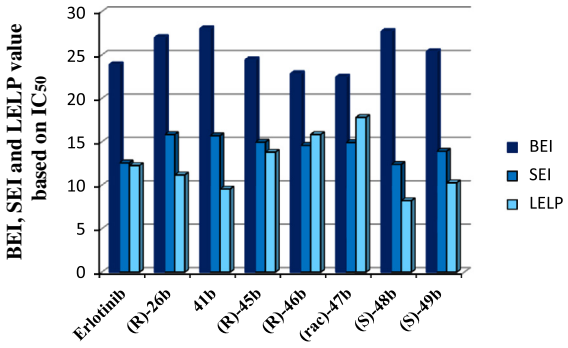

Fig. 7. Binding efficiency (BEI), surface efficiency index (SEI), and ligand-efficiency-dependent lipophilicity (LELP) for derivatives having variable R_1-group.

lipohilicity. Values below 10 are preferable. In terms of LELP, (*S*)-**48b** was analysed to have a slightly better profile than (*R*)-**26b**, **41b** and Erlotinib. As a result of these analysis further development was based on the scaffolds (*R*)-**26**, **41** and (*S*)-**48**.

3.3.2. Fine tuning of activity towards EGFR-TK

The fine tuning of potency was started by studying variations in the 6-aryl group (Fragment B), with (*R*)-1-phenylethanamine as the 4-amino group. The aromatic substitution pattern in the 6-aryl group was largely based on our recent finding in the corresponding thienopyrimidines (Bugge et al., 2014), in which high EGFR-TK potency was observed when having ether and hydroxyl substituents attached to the aromatic ring. The compounds analysed for EGFR-TK potency, and the previously made reference compounds (*R*)-**26a** and (*R*)-**34a** (Section 2.3.1), (*R*)-**26c-d** and (*R*)-**34i** (Kaspersen et al., 2011) and (*R*)-**26i** (PKI-166) (Kaspersen et al., 2011; Caravatti et al., 2001; Hoekstra et al., 2005) are shown in Fig. 8.

The inhibitory potency of the compounds increased considerably by having a hydroxymethyl group in *para* or *meta* position, and compounds (*R*)-**26k** and (*R*)-**26l** both had IC_{50} values of 0.3 nM. Improvements in IC_{50} values were also seen for the *ortho* derivatives (*R*)-**26e**, (*R*)-**26j** and the *meta* hydroxyl compound (*R*)-**26h**. The *ortho* hydroxyl derivative (*R*)-**26f** was considerable less active. The root cause of the drop in activity is somewhat unclear, but might be due to internal hydrogen bonding with the pyrrolo nitrogen likely to affect conformation of the 6-aryl group.

Data for the previously described compounds (*R*)-**26c-d** visualise important structure–activity information for the 6-aryl group. Whereas, the small fluorine group has only minor impact on potency, the larger and more lipophilic bromine substituent reduced the activity more profoundly. The EGFR-TK inhibitory activity was less affected by fluorine substitution in *para* position of Fragment A as indicated by data for compound (*R*)-**34a** and (*R*)-**34i**.

Further it was attempted to improve antagonist activity by merging potency inducing structural groups into one molecule. Substructure selection in Fragment A was based on a compromise between potency and calculated druglike properties. Therefore, scaffolds with the more lipophilic (*R*)-1-phenylethanamine group, (*R*)-**26**, and the more polar hydroxymethyl group, (*S*)-**48**, were focused. Additionally, selected fluorinated derivatives, and two benzylamine based compounds were included due to their highly active EGFR-TK inhibitory properties. The compounds identified alongside their precursor molecules are shown in Fig. 9.

Ten additional inhibitors with IC_{50} values below 1 nM were identified. The most active compounds possess the 4-hydroxymethyl-2-methoxyphenyl group at C-6 (Fragment B). The effect of substituents on potency was not additive indicating that enthalpy/entropy compensating effects come into play. Generally, somewhat higher IC_{50} values (lower activity) were noted for the benzylamine fragment **41** as compared to (*R*)-**26** and (*S*)-**48**. The docked structure of (*S*)-**48n** is shown in Fig. 10, and the main interactions between the ligand and the ATP binding site of EGFR-TK is highlighted in Fig. 11. Compound (*S*)-**48n** is indicated to bind similar to that of (*S*)-**48b** (Fig. 5), but an additional hydrogen bond from the hydroxymethyl group to Leu718 was seen explaining the increased potency. Additionally, both the secondary amine function and N-3 of the pyrimidine unit were indicated to bind to water molecules.

The druglike properties of compounds having IC_{50} values below 0.7 nM were calculated as described in Section 3.3.1. Due to the potential toxicity of the aldehydes (*R*)-**26m**, **41m**, (*S*)-**48m**, and (*S*)-**60m**, these were not included. The LE values shown in Fig. 12 revealed that all compounds except (*S*)-**60n** have a more favourable profile than Erlotinib.

The calculated BEI, SEI and LELP values are shown in Fig. 13. BEI values follows the trends of LE, were only (*S*)-**60n** has lower binding efficiency than Erlotinib.

Erlotinib has similar surface efficiency index as (*R*)-**26l** and (*S*)-**48b**, while the other pyrrolopyrimidines have lower values, which indicates that the compounds might be too polar. On the other hand these properties allow all compounds to have ligand-efficiency-dependent lipophilicity (LELP) within the target area, while Erlotinib is indicated to be too lipophilic.

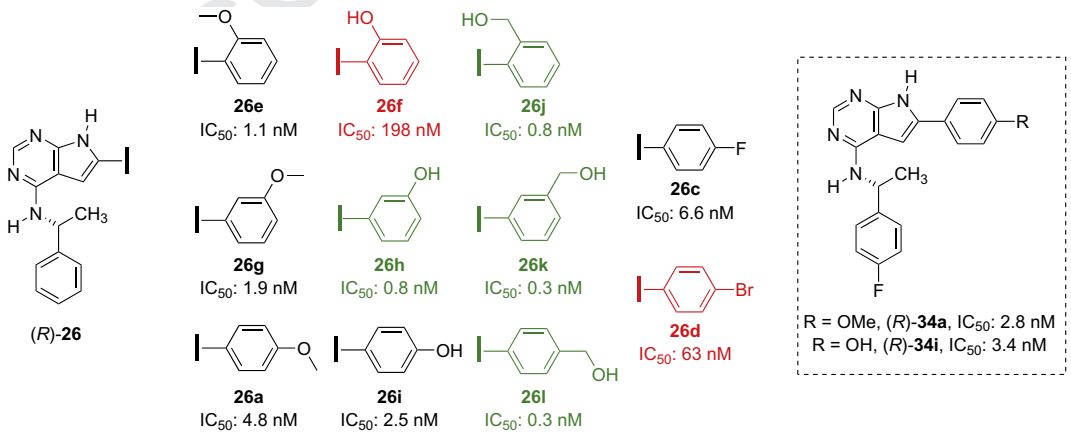

Fig. 8. Effect of structural variations in Fragment B on EGFR-TK potency. The data, standard deviations and single point measurement are shown in Supporting information.

Please cite this article in press as: Kaspersen, S.J., et al. Identification of new 4-*N*-substituted 6-aryl-7*H*-pyrrolo[2,3-*d*] pyrimidine-4-amines as highly potent EGFR-TK inhibitors with Src-family activity. Eur. J. Pharm. Sci. (2014), http://dx.doi.org/10.1016/j.ejps.2014.04.011

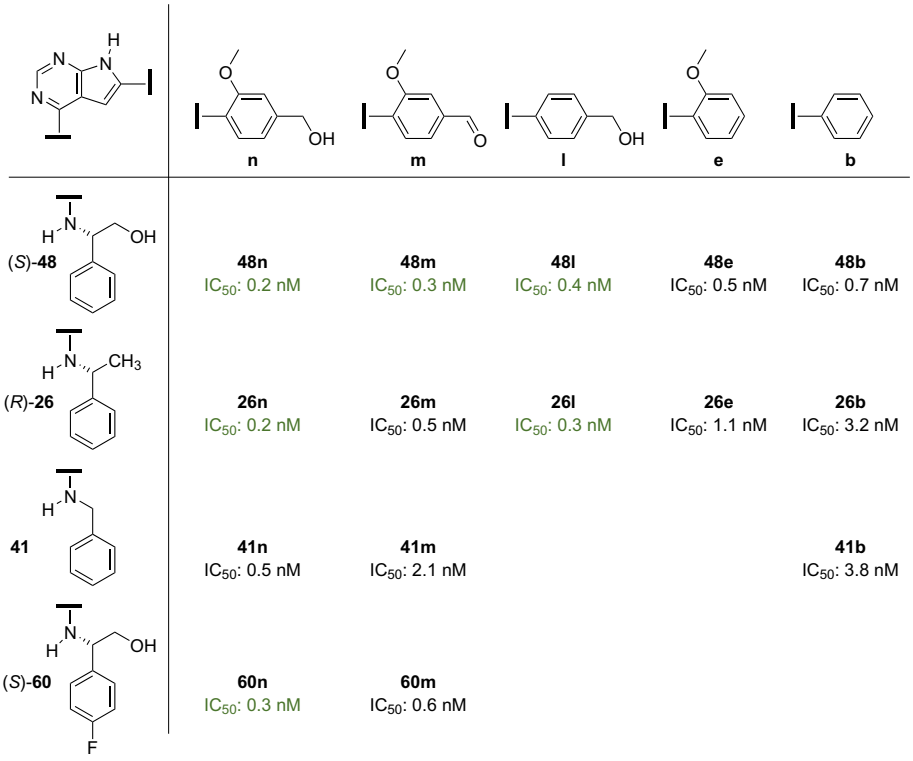

Fig. 9. Combination of fragments to increase EGFR-TK potency. Compounds (*R*)-**26b**, **41b** and (*S*)-**48b** are included as reference. The IC_{50} data, standard deviations and single point data for these and some additional compounds are shown in Supporting information.

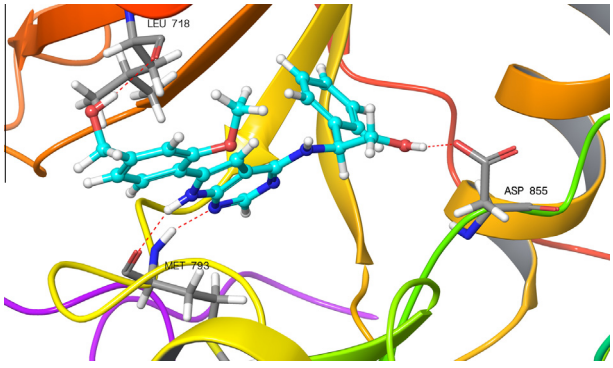

Fig. 10. Binding of compound (*S*)-**48n** to the EGFR-TK ATP binding site based on the crystal structure 2J6M (Yun et al., 2007). The compound is indicated to engage in hydrogen bonding via the hydroxymethyl group to Asp855 in the DFG motif, by N-1 to back-bond NH of Met793 and by the *para*-hydroxymethyl group to Leu718.

3.3.3. Structure–activity relationships

A summary of the structure–activity relationship seen base on this and our previous study (Kaspersen et al., 2011) is shown in Fig. 14.

By modifying Fragment A the activity was increased by having hydroxymethyl or methoxymethyl as R_1, which is explained by hydrogen interactions with Thr854 and Asp855 in the DFG motif (Figs. 10 and 11). The insertion of bulky groups as R_1 does not affect the activity to a large extent. However, when bulky substituents were placed in *para* position of the aromatic ring (R_2), a dramatic drop in potency was seen. This is explained by size limitations in this part of the binding pocket. In the aromatic part of Fragment A substitution seems to be better tolerated in *ortho* than in *meta* position, although there is limited number of data for *meta* substituted derivatives. As opposed to the thienopyrimidine based analogues (Bugge et al., 2014), fluorine substitution was generally well tolerated in the aromatic part. This indicates a slightly different binding mode.

Substitution of the 6-aryl group (Fragment B) increased EGFR-TK activity especially when having a hydroxymethyl group in the *para* or *meta* position. Modelling indicate this to be due to a hydrogen bonding interaction with Leu718 (Figs. 10 and 11). For aromatic methoxy substituents the activity increased in the order *para* < *meta* < *ortho*. In contrast, the *ortho* hydroxy analogue had a low potency, whereas the *meta*- and *para* hydroxy substituted derivatives were highly active. Possibly, this is due to conformational effects caused by intramolecular hydrogen bonding with the pyrrole-NH. The large lipophilic bromine substituent was not tolerated in *para* position as also noted for bulky lipophilic groups in the thienopyrimidine series of compounds (Bugge et al., 2014).

3.3.4. Activity towards EGFR mutants

The most potent compounds identified in enzymatic assays towards wild-type EGFR-TK were also evaluated towards the $EGFR^{L858R}$, $EGFR^{L861Q}$ and $EGFR^{T790M}$ mutants. The key results are compiled in Table 2.

All the compounds assayed were found very potent towards both the $EGFR^{L858R}$ and $EGFR^{L861Q}$ mutants. On average, as compared to the wild-type EGFR-TK assay, somewhat higher IC_{50} values were seen towards $EGFR^{L858R}$, while mostly similar IC_{50} values were noted in the case of $EGFR^{L861Q}$. As expected for reversible inhibitors, testing towards the $EGFR^{T790M}$ mutant only revealed activity in the μM range (Kitagawa et al., 2013). Compounds (*R*)-**26l** and **41** showed lower inhibitory potency towards $EGFR^{T790M}$ as compared to the other drug candidates. Although a more elaborate study is needed to understand the SAR relationship, the limited data suggests that the activity is increased by having a hydroxymethyl group at the chiral centre and at the *para* position of the 6-aryl ring. An *ortho*-methoxy group on the 6-aryl ring is also

Please cite this article in press as: Kaspersen, S.J., et al. Identification of new 4-*N*-substituted 6-aryl-7*H*-pyrrolo[2,3-*d*] pyrimidine-4-amines as highly potent EGFR-TK inhibitors with Src-family activity. Eur. J. Pharm. Sci. (2014), http://dx.doi.org/10.1016/j.ejps.2014.04.011

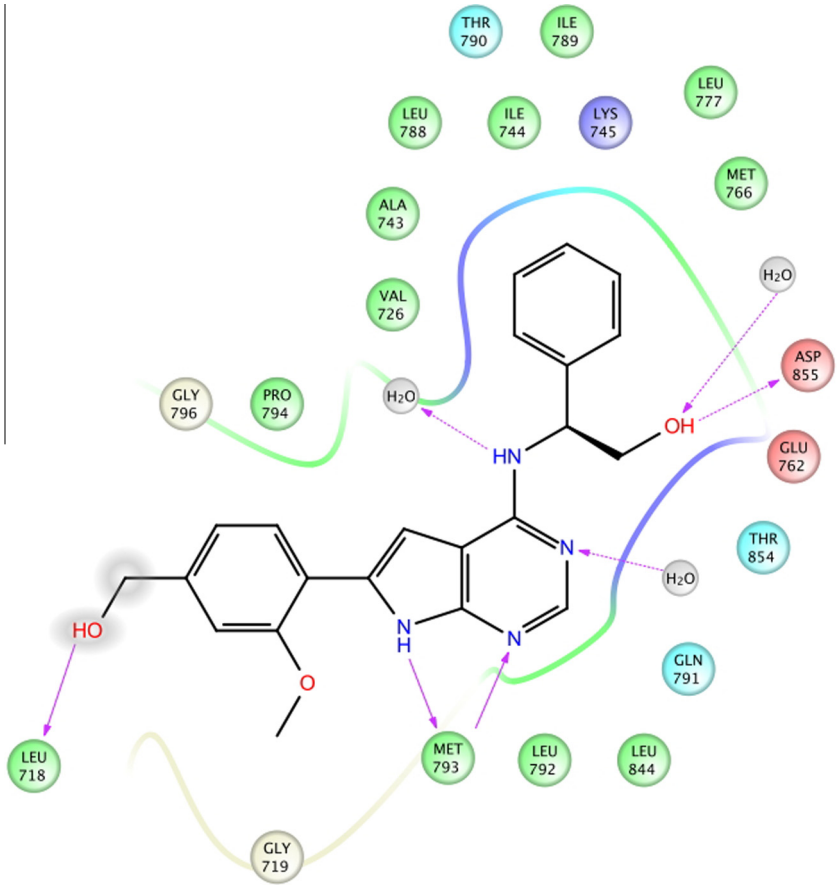

Fig. 11. Interaction map highlighting amino acids within 5 Å distance from the docked ligand. The colours indicate residue type: green – lipophilic residues; red – acidic residues; blue – polar residues; purple – basic residues. The protein "pocket" is displayed with a line around the ligand, coloured with the colour of the nearest protein residue. Ligand atoms that are exposed to solvent are marked with grey spheres. (For interpretation of the references to colour in this figure legend, the reader is referred to the web version of this article.)

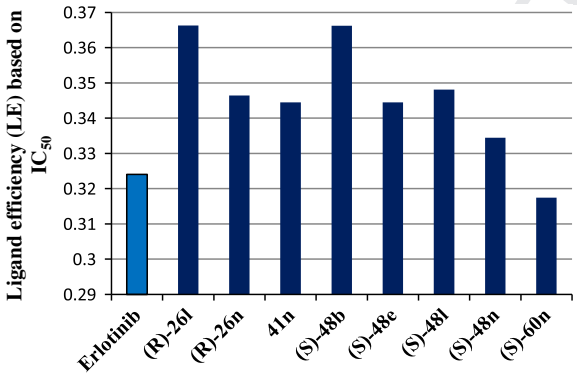

Fig. 12. Ligand efficiency (LE) for derivatives (*R*)-**26l**, (*R*)-**26n**, (*S*)-**41n**, (*S*)-**48b**, (*S*)-**48e**, (*S*)-**48l**, (*S*)-**48n** and (*S*)-**60n** compared to Erlotinib.

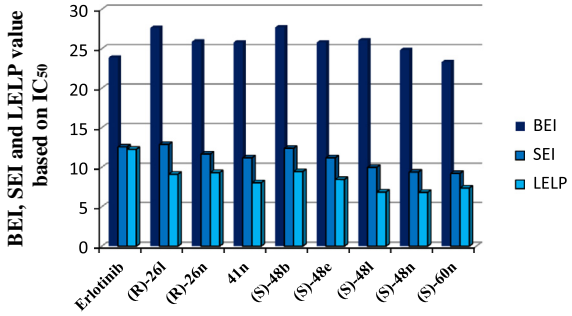

Fig. 13. Binding efficiency (BEI), surface efficiency index (SEI), and ligand-efficiency-dependent lipophilicity (LELP) for derivatives (*R*)-**26l**, (*R*)-**26n**, **41n**, (*S*)-**48b**, (*S*)-**48l**, (*S*)-**48n** and (*S*)-**60n** compared to Erlotinib.

favourable. As in the wild-type EGFR-TK assay, compounds lacking one or more of these groups display lower activity towards $EGFR^{T790M}$. Docking of (*R*)-**26l**, **41n** and the more potent (*S*)-**48n** in $EGFR^{T790M}$ confirmed this as similar binding mode and interactions were seen as in wild-type EGFR-TK.

3.3.5. Kinase profiling

As the ATP binding site of kinases is somewhat conserved, other kinases might be inhibited as well. This could be problematic in terms of off-target toxic effects, but could also represent an opportunity to inhibit several misregulated kinase signalling pathways.

Thus, the same eight selected pyrrolopyrimidines were tested towards an extended panel of 53 kinases, and compared with the corresponding profile of Erlotinib. As this represent a huge amount of data it is convenient to quantify the selectivity by the use of Gini plots and Gini coefficients (Graczyk, 2007). Overall the compounds displayed a selectivity profile similar to Erlotinib. The Gini plot, where the cumulative fraction of kinases is plotted towards the cumulative fraction of total inhibition, for Erlotinib, the most selective compound **41n** and the least selective compound (*S*)-**48l**, is shown in Fig. 15.

Please cite this article in press as: Kaspersen, S.J., et al. Identification of new 4-*N*-substituted 6-aryl-7*H*-pyrrolo[2,3-*d*] pyrimidine-4-amines as highly potent EGFR-TK inhibitors with Src-family activity. Eur. J. Pharm. Sci. (2014), http://dx.doi.org/10.1016/j.ejps.2014.04.011

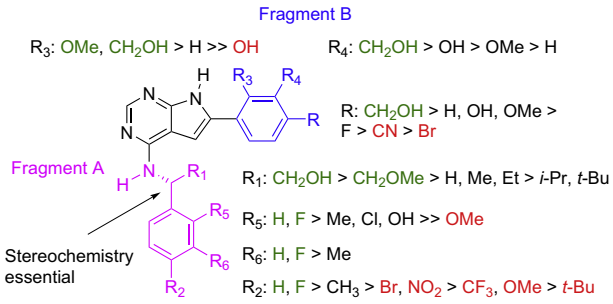

Fig. 14. Structure–activity relationships identified in this and previous study (Kaspersen et al., 2011). Colour code: green: induce potency; black: minor effects; red: reduce potency. (For interpretation of the references to colour in this figure legend, the reader is referred to the web version of this article.)

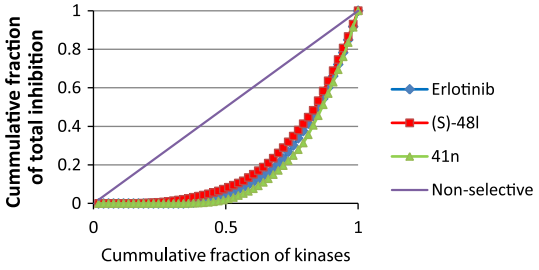

Fig. 15. Gini plots based on % inhibition of 53 kinases at 500 nM for Erlotinib, **41n** and (*S*)-**48l**. The cumulative fraction of kinases is plotted towards the cumulative fraction of total inhibition. Gini coefficients: Erlotinib: 0.628; **41n**: 0.665; (*S*)-**48l**: 0.577. A profile represented by the straight line would be non-selective.

However, closer inspection of the data showed that Erlotinib and the pyrrolopyrimidines had some major differences, see Table 3. Erlotinib was found to be a better inhibitor of the kinase insert domain receptor (KDR) and the RET proto-oncogene receptor tyrosine kinase (RET) than the pyrrolopyrimidines. On the other hand, the pyrrolopyrimidines had higher degree of inhibition towards colony stimulating factor 1 receptor kinase (CSF1R), and the Src-family of kinase including especially feline Gardner-Rasheed sarcoma viral oncogene homolog (FGR), v-src avian sarcoma (Src) and Yamaguchi sarcoma viral oncogene homolog (YES1) kinases. Both CSF1R (Krol et al., 2013; Xu et al., 2013) and Src-family of kinase (Kim et al., 2009) are potential targets in cancer therapy. The HER2 and HER4 inhibition potency were found rather similar, though in cases of compounds (*R*)-**26n** and (*S*)-**48n** higher HER preference was seen.

3.4. Cellular assays

Eight of the new pyrrolopyrimidine based EGFR-TK inhibitors were evaluated in two genetically modified model cells Ba/F3-EGFR^{L858R} and Ba/F3-EGFR^{T790M}, and four human cancer cell lines including A-431 (epidermoid carcinoma), AU-565 (breast adenocarcinoma), K-562 (leukaemia) and C-33A (cervix carcinoma). The results are shown in Table 4.

The Ba/F3-EGFR cells (Kancha et al., 2009) display growth and survival dependent on EGFR signalling. Cell proliferation study with Ba/F3-EGFR^{L858R} cells using the XTT assay proved to be a highly sensitive test system for evaluating the EGFR-TK inhibitors. Of the eight compounds assayed, seven were highly active with IC_{50} values in the range of 80–172 nM, while the benzylamine based compound **41n**, was less potent than the other derivatives. Compounds (*R*)-**26n**, (*S*)-**48n** and (*S*)-**60n** sharing the same aryl moiety, and the *para* hydroxymethyl derivative (*R*)-**26l** were found more active than Erlotinib. None of the compounds inhibited proliferation of the Ba/F3-EGFR^{T790M} cell line indicating that the cytotoxicity is mainly due to EGFR^{L858R} inhibition. The A-431 cells, which overexpress EGFR (Ullrich et al., 1984; Bravo et al., 1985), were also sensitive towards the compounds tested. Interestingly, the structure of the R_1 group at the stereocentre was found to be of higher importance than was the case in the Ba/F3-EGFR^{L858R} system. Higher activity was noted when having the hydroxymethyl substituent at the stereocenter than was the case for the methyl or unsubstituted derivatives. A-431 cells also contain HER2 (Meira et al., 2011; Moasser et al., 2001) and are known to be sensitive to Src inhibitors (Donnini et al., 2007). However, the kinase selectivity data does not support inhibition of these kinases to be the cause of the observed difference in cell proliferation seen among the compounds. Testing towards the AU-565 cell line, which possesses low level of EGFR, but overexpress HER2, HER3,

Table 2
IC_{50} values (nM) of pyrrolopyrimidines towards EGFR^{L858R} and EGFR^{L861Q} (nM) and activity at 50 μM towards EGFR^{T790M} (inhibition data for other derivatives are shown in the Supporting information).

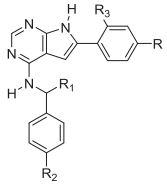

Compounds	R_1	R	R_2	R_3	EGFR^{L858R} (IC_{50}, nM)[a]	EGFR^{L861Q} (IC_{50}, nM)[a]	EGFR^{T790M} (% inhibition)[b]
(*R*)-**26l**	CH_3	CH_2OH	H	H	0.8 ± 0.1	0.3 ± 0.1	44
(*R*)-**26n**	CH_3	CH_2OH	H	OMe	0.4 ± 0.0	0.2 ± 0.0	95
41n	H	CH_2OH	H	OMe	0.8 ± 0.0	0.4 ± 0.1	66
(*S*)-**48b**	CH_2OH	H	H	H	1.3 ± 0.1	1.0 ± 0.2	91
(*S*)-**48e**	CH_2OH	H	H	OMe	0.1 ± 0.0	0.2 ± 0.0	94
(*S*)-**48l**	CH_2OH	CH_2OH	H	H	0.4 ± 0.0	0.2 ± 0.0	84
(*S*)-**48n**	CH_2OH	CH_2OH	H	OMe	0.4 ± 0.0	0.3 ± 0.0	97
(*S*)-**60n**	CH_2OH	CH_2OH	F	OMe	0.6 ± 0.0	0.3 ± 0.0	97
Erlotinib	[c]				0.6 ± 0.1	0.5 ± 0.0	95

[a] IC_{50} value and standard deviation based on duplicate measurement.
[b] Percent inhibition at 50 μM concentration, average of duplicate measurements.
[c] For structure see Fig. 1.

Table 3
Activity (% inhibition) of eight pyrrolopyrimidines and Erlotinib towards selected kinases at 500 nM test concentration.

Kinase	**Erlotinib**	(*R*)-**26l**	(*R*)-**26n**	**41n**	(*S*)-**48b**	(*S*)-**48e**	(*S*)-**48l**	(*S*)-**48n**	(*S*)-**60n**
ABL1	75	73	75	77	65	50	84	68	73
CSF1R (FMS)	38	92	87	92	88	79	90	82	75
ERBB2 (HER2)	52	53	76	58	53	53	48	64	59
ERBB4 (HER4)	78	25	70	49	51	79	71	87	76
FGR	42	82	92	86	73	74	84	89	79
FRK (PTK5)	16	40	46	25	33	36	50	58	55
FYN	−13	34	29	31	27	27	44	42	46
HCK	18	37	30	25	29	30	46	38	43
KDR (VEGFR2)	70	nd[a]	31	22	28	15	38	34	35
LCK	49	33	1	13	13	17	36	37	36
LYN A	68	65	78	68	47	52	74	73	66
LYN B	68	67	81	75	60	64	70	77	69
RET	64	9	7	17	14	15	26	19	32
SRC	42	61	75	66	59	59	74	66	63
YES1	29	69	73	67	65	68	81	72	68
HER2/HER4 average	65	39	73	54	52	66	60	76	68
Src average	38	56	57	54	47	49	64	62	58

[a] Not determined.

Table 4
Summary of cell proliferation data (IC_{50}) of pyrrolopyrimidines towards Ba/F3-$EGFR^{L858R}$, A-431, AU-565, C-33A and K-562. Curve data are shown in Supporting information.

	Ba/F3-$EGFR^{L858R}$ nM ($n = 3$)	A-431 μM ($n = 3$)	AU-565 μM ($n = 2$)	C-33A μM ($n = 2$)	K-562 μM ($n = 3$)
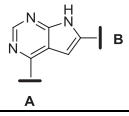					
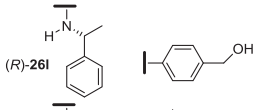 (*R*)-**26l**	80 ± 9	1.2 ± 0.5	>31	0.8 ± 0.1	>100
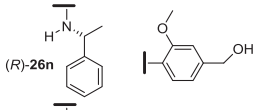 (*R*)-**26n**	99 ± 27	0.8 ± 0.4	2.9 ± 0.5	0.8 ± 0.2	9.5 ± 0.5
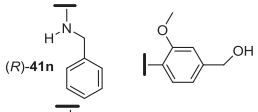 (*R*)-**41n**	>200	0.8 ± 0.1	>31	1.1 ± 0.3	>100
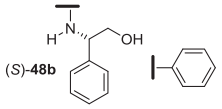 (*S*)-**48b**	127 ± 29	0.3 ± 0.1	2.5 ± 0.4	0.7 ± 0.0	15 ± 2
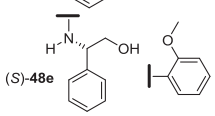 (*S*)-**48e**	134 ± 22	0.4 ± 0.1	1.2 ± 0.1	0.8 ± 0.0	17 ± 1
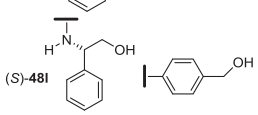 (*S*)-**48l**	172 ± 46	0.5 ± 0.1	2.8 ± 0.1	0.5 ± 0.0	18 ± 2
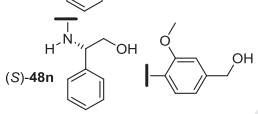 (*S*)-**48n**	70 ± 22	0.5 ± 0.3	1.9 ± 0.2	0.4 ± 0.0	16 ± 2
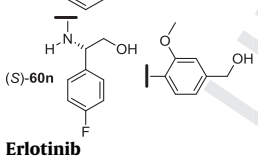 (*S*)-**60n**	83 ± 13	0.8 ± 0.1	3.4 ± 0.2	0.8 ± 0.1	29 ± 1
Erlotinib	142 ± 65	0.4 ± 0.1	3.3 ± 0.6	0.9 ± 0.0	55 ± 9

HER4 (Bacus et al., 1992; Goestring et al., 2012; Sebban et al., 2013), revealed that six of the compounds had comparable or better activity than Erlotinib. Best activity was again observed for compounds based on 2-amino-2-phenylethan-1-ol as C-4 substituent (Fragment A). The most potent compound identified was (*S*)-**48e** having an *ortho*-methoxy group at the 6-aryl ring. Compound (*R*)-**26l** and benzyl derivative **41n** had low inhibitory effect. The C-33A cell line, which also possesses low level of EGFR, but contains HER2 (Meira et al., 2011), was found to be highly sensitive towards all the pyrrolopyrimidines. Seven of the compounds tested

Please cite this article in press as: Kaspersen, S.J., et al. Identification of new 4-*N*-substituted 6-aryl-7*H*-pyrrolo[2,3-*d*] pyrimidine-4-amines as highly potent EGFR-TK inhibitors with Src-family activity. Eur. J. Pharm. Sci. (2014), http://dx.doi.org/10.1016/j.ejps.2014.04.011

had comparable or better activity that Erlotinib. K-562 is a leukaemia Bcr-Abl positive cell line, in which cell proliferation also has been correlated with Src inhibition (Wilson et al., 2002). K-562 was considerable less sensitive towards all the compounds than the other cell lines. Further, the data suggests that Erlotinib, the hydroxymethyl derivative (*R*)-**26l** and the benzylic **41n** had a cytostatic rather than a cytotoxic effect. Derivative (*R*)-**26n** was analysed most active with an IC_{50} of 9.5 μM.

4. Conclusion

Based on two complementary synthetic routes a series of new pyrrolopyrimidine derivatives have been prepared and evaluated as epidermal growth factor receptor tyrosine kinase inhibitors in enzymatic studies. Tuning of activity was done by a step wise approach by combining activity inducing groups at the C-4 and C-6 positions of the pyrrolopyrimidine scaffold. Overall, eight compounds, with promising druglike properties, were identified. The highest enzymatic inhibitory potency was obtained when having polar hydroxymethyl substituents both at the stereocenter and in the 6-aryl group. Moreover, kinase profiling identified that the new pyrrolopyrimidines also possess significant Src-kinase family and CSF1R activity potentially useful in a therapeutic setting. Eight compounds were further evaluated and compared with Erlotinib in six cell systems including the Ba/F3-$EGFR^{L858R}$ and Ba/F3-$EGFR^{T790M}$ model cells, and A-431, AU-565, C-33A and K-562. Several of the identified molecules compares favourably with Erlotinib in these cancer cell models.

Acknowledgements

Susana Villa Gonzalez is acknowledged for the HRMS experiments. Roger Aarvik, Christopher Sørum and Veronica Willassen are also acknowledged for their contribution. Prof. Dr. Justus Duyster and Dr. Nikolas von Bubnoff, Technical University of Munich, Munich, Germany kindly provided EGFR Ba/F3 cells. Anders Jahres foundation and Technology Transfer Office (TTO-NTNU Trondheim) are thanked for financial support.

Appendix A. Supplementary material

Supplementary data associated with this article can be found, in the online version, at http://dx.doi.org/10.1016/j.ejps.2014.04.011.

References

Abad-Zapatero, C., 2007. Ligand efficiency indices for effective drug discovery. Expert Opin. Drug Discov. 2, 469–488.
Abad-Zapatero, C., Metz, J.T., 2005. Ligand efficiency indices as guideposts for drug discovery. Drug Discov. Today 10, 464–469.
Bacus, S.S., Stancovski, I., Huberman, E., Chin, D., Hurwitz, E., Mills, G.B., Ullrich, A., Sela, M., Yarden, Y., 1992. Tumor-inhibitory monoclonal antibodies to the HER-2/Neu receptor induce differentiation of human breast cancer cells. Cancer Res. 52, 2580–2589.
Barf, T., Kaptein, A., 2012. Irreversible protein kinase inhibitors: balancing the benefits and risks. J. Med. Chem. 55, 6243–6262.
Böhm, H., Banner, D., Bendels, S., Kansy, M., Kuhn, B., Muller, K., Obst-Sander, U., Stahl, M., 2004. Fluorine in medicinal chemistry. ChemBioChem 5, 637–643.
Bravo, R., Burckhardt, J., Curran, T., Muller, R., 1985. Stimulation and inhibition of growth by EGF in different A431 cell clones is accompanied by the rapid induction of c-fos and c-myc proto-oncogenes. EMBO J. 4, 1193–1197.
Bugge, S., Kaspersen, S.J., Larsen, S., Nonstad, U., Bjørkøy, G., Sundby, E., Hoff, B.H., 2014. Structure-activity study leading to identification of a highly active thienopyrimidine based EGFR inhibitor. Eur. J. Med. Chem. 75, 354–374.
Caravatti, G., 2004. New 7H-pyrrolo[2,3-d]pyrimidines inhibiting ErbB and VEGF receptor tyrosine kinases. In: Abstracts, 36th Central Regional Meeting of the American Chemical Society, Indianapolis, IN, United States.
Caravatti, G., Bruggen, J., Buchdunger, E., Cozens, R., Furet, P., Lydon, N., O'Reilly, T., Traxler, P., 2001. Pyrrolo[2,3-d]pyrimidine and pyrazolo[3,4-d]pyrimidine derivatives as selective inhibitors of the EGF receptor tyrosine kinase. ACS Symp. Ser. 796, 231–244.
Carmi, C., Mor, M., Petronini, P.G., Alfieri, R.R., 2012. Clinical perspectives for irreversible tyrosine kinase inhibitors in cancer. Biochem. Pharmacol. 84, 1388–1399.
Chong, C.R., Jaenne, P.A., 2013. The quest to overcome resistance to EGFR-targeted therapies in cancer. Nat. Med. 19, 1389–1400.
Donnini, S., Monti, M., Castagnini, C., Solito, R., Botta, M., Schenone, S., Giachetti, A., Ziche, M., 2007. Pyrazolo-pyrimidine-derived c-Src inhibitor reduces angiogenesis and survival of squamous carcinoma cells by suppressing vascular endothelial growth factor production and signaling. Int. J. Cancer 120, 995–1004.
Engelhardt, H., Boehmelt, G., Kofink, C., Kuhn, D., McConnell, D., Stadtmueller, H. Preparation of pyrimidinonecarboxylic acid amides with antiproliferative activity, WO 2010007114, 21–1–2010.
Ertl, P., Rohde, B., Selzer, P., 2000. Fast calculation of molecular polar surface area as a sum of fragment-based contributions and its application to the prediction of drug transport properties. J. Med. Chem. 43, 3714–3717.
Induced Fit Docking Protocol 2013-3, 2013. Glide Version 6.1, Prime Version 3.4, Schrödinger, LLC, New York, NY.
Goestring, L., Malm, M., Hoeiden-Guthenberg, I., Frejd, F.Y., Staahl, S., Loefblom, J., Gedda, L., 2012. Cellular effects of HER3-specific affibody molecules. PLoS One 7, e40023.
Graczyk, P.P., 2007. Gini coefficient: a new way to express selectivity of kinase inhibitors against a family of kinases. J. Med. Chem. 50, 5773–5779.
Grotzfeld, R.M., Patel, H.K., Mehta, S.A., Milanov, Z.V., Lai, A.G., Lockhart, D.J. Pyrrolopyrimidine Derivatives and Analogs and their use in the Treatment and Prevention of Diseases, US 2005153989, 13–1–2005.
Hebert-Chatelain, E., 2013. Src kinases are important regulators of mitochondrial functions. Int. J. Biochem. Cell Biol. 45, 90–98.
Hoekstra, R., Dumez, H., Eskens Ferry, A.L.M., van der, G.A., Planting Andre, S.T., de, H.G., Sizer, K.C., Ravera, C., Vaidyanathan, S., Bucana, C., Fidler, I.J., van Oosterom, A.T., Verweij, J., 2005. Phase I and pharmacologic study of PKI166, an epidermal growth factor receptor tyrosine kinase inhibitor, in patients with advanced solid malignancies. Clin. Cancer Res. 11, 6908–6915.
Hopkins, A.L., Groom, C.R., Alex, A., 2004. Ligand efficiency: a useful metric for lead selection. Drug Discov. Today 9, 430–431.
Hynes, N.E., MacDonald, G., 2009. ErbB receptors and signaling pathways in cancer. Curr. Opin. Cell Biol. 21, 177–184.
Irwin, M.E., Bohin, N., Boerner, J.L., 2011. Src family kinases mediate epidermal growth factor receptor signaling from lipid rafts in breast cancer cells. Cancer Biol. Ther. 12, 718–726.
Kancha, R.K., von Bubnoff, N., Peschel, C., Duyster, J., 2009. Functional analysis of epidermal growth factor receptor (EGFR) mutations and potential implications for EGFR targeted therapy. Clin. Cancer Res. 15, 460–467.
Kaspersen, S.J., Sørum, C., Willassen, V., Fuglseth, E., Kjøbli, E., Bjørkøy, G., Sundby, E., Hoff, B.H., 2011. Synthesis and in vitro EGFR (ErbB1) tyrosine kinase inhibitory activity of 4-N-substituted 6-aryl-7H-pyrrolo[2,3-d]pyrimidine-4-amines. Eur. J. Med. Chem. 46, 6002–6014.
Kaspersen, S.J., Sundby, E., Charnock, C., Hoff, B.H., 2012. Activity of 6-aryl-pyrrolo[2,3-*d*]pyrimidine-4-amines to *Tetrahymena*. Bioorg. Chem. 44, 35–41.
Keserue, G.M., Makara, G.M., 2009. The influence of lead discovery strategies on the properties of drug candidates. Nat. Rev. Drug Discov. 8, 203–212.
Kim, L.C., Song, L., Haura, E.B., 2009. Src kinases as therapeutic targets for cancer. Nat. Rev. Clin. Oncol. 6, 587–595.
Kinzel, T., Zhang, Y., Buchwald, S.L., 2010. A new palladium precatalyst allows for the fast Suzuki–Miyaura coupling reactions of unstable polyfluorophenyl and 2-heteroaryl boronic acids. J. Am. Chem. Soc. 132, 14073–14075.
Kitagawa, D., Yokota, K., Gouda, M., Narumi, Y., Ohmoto, H., Nishiwaki, E., Akita, K., Kirii, Y., 2013. Activity-based kinase profiling of approved tyrosine kinase inhibitors. Genes Cells 18, 110–122.
Koehler, J., Schuler, M., 2013. Afatinib, erlotinib and gefitinib in the first-line therapy of EGFR mutation-positive lung adenocarcinoma: a review. Onkologie 36, 510–518.
Krol, M., Majchrzak, K., Mucha, J., Homa, A., Bulkowska, M., Jakubowska, A., Karwicka, M., Pawalowski, K.M., Motyl, T., 2013. CSF-1R as an inhibitor of apoptosis and promoter of proliferation, migration and invasion of canine mammary cancer cells. BMC Vet. Res. 9, 65, 13.
Lainey, E., Wolfromm, A., Sukkurwala, A.Q., Micol, J., Fenaux, P., Galluzzi, L., Kepp, O., Kroemer, G., 2013. EGFR inhibitors exacerbate differentiation and cell cycle arrest induced by retinoic acid and vitamin D3 in acute myeloid leukemia cells. Cell Cycle 12, 2978–2991.
Landi, L., Cappuzzo, F., 2013. Irreversible EGFR-TKIs: dreaming perfection. Transl. Lung Cancer Res. 2, 40–49.
Leeson, P.D., Springthorpe, B., 2007. The influence of drug-like concepts on decision-making in medicinal chemistry. Nat. Rev. Drug Discov. 6, 881–890.
Lu, X.L., Liu, X.Y., Cao, X., Jiao, B.H., 2012. Novel patented Src kinase inhibitor. Curr. Med. Chem. 19, 1821–1829.
Meanwell, N.A., 2011. Improving drug candidates by design: a focus on physicochemical properties as a means of improving compound disposition and safety. Chem. Res. Toxicol. 24, 1420–1456.
Meira, D.D., Almeida, V.H., Mororo, J.S., Caetano, M.S., Nobrega, I.P., Batista, D., Sternberg, C., Ferreira, C.G., 2011. Efficient blockade of Akt signaling is a determinant factor to overcome resistance to matuzumab. Mol. Cancer 10, 151.
Moasser, M.M., Basso, A., Averbuch, S.D., Rosen, N., 2001. The tyrosine kinase inhibitor ZD1839 ("Iressa") inhibits HER2-driven signaling and suppresses the growth of HER2-overexpressing tumor cells. Cancer Res. 61, 7184–7188.

Nedergaard, M.K., Hedegaard, C.J., Poulsen, H.S., 2012. Targeting the epidermal growth factor receptor in solid tumor malignancies. BioDrugs 26, 83–99.

Park, Y.W., Younes, M.N., Jasser, S.A., Yigitbasi, O.G., Zhou, G., Bucana, C.D., Bekele, B.N., Myers, J.N., 2005. AEE788, a dual tyrosine kinase receptor inhibitor, induces endothelial cell apoptosis in human cutaneous squamous cell carcinoma xenografts in nude mice. Clin. Cancer Res. 11, 1963–1973.

Park, J.H., Liu, Y., Lemmon, M.A., Radhakrishnan, R., 2012. Erlotinib binds both inactive and active conformations of the EGFR tyrosine kinase domain. Biochem. J. 448, 417–423.

Peng, Y.H., Shiao, H.Y., Tu, C.H., Liu, P.M., Hsu, J.T.-A., Amancha, P.K., Wu, J.S., Coumar, M.S., Chen, C.H., Wang, S.Y., Lin, W.H., Sun, H.Y., Chao, Y.S., Lyu, P.C., Hsieh, H.P., Wu, S.Y., 2013. Protein kinase inhibitor design by targeting the Asp-Phe-Gly (DFG) motif: the role of the DFG motif in the design of epidermal growth factor receptor inhibitors. J. Med. Chem. 56, 3889–3903.

Pollok, B.A., Hamman, B.D., Rodems, S.M., Makings, L.R., Optical Probes and Assays, WO 2000066766 A1, 5–5–2000.

Sebban, S., Farago, M., Gashai, D., Ilan, L., Pikarsky, E., Ben-Porath, I., Katzav, S., 2013. Vav1 fine tunes p53 control of apoptosis versus proliferation in breast cancer. PLoS One 8, e54321.

Sequist, L.V., Besse, B., Lynch, T.J., Miller, V.A., Wong, K.K., Gitlitz, B., Eaton, K., Zacharchuk, C., Freyman, A., Powell, C., Ananthakrishnan, R., Quinn, S., Soria, J.C., 2010. Neratinib, an irreversible Pan-ErbB, receptor tyrosine kinase inhibitor: results of a phase II trial in patients with advanced non-small-cell lung cancer. J. Clin. Oncol. 28, 3076–3083.

Sgambato, A., Casaluce, F., Maione, P., Rossi, A., Rossi, E., Napolitano, A., Palazzolo, G., Bareschino, M.A., Schettino, C., Sacco, P.C., Ciadiello, F., Gridelli, C., 2012. The role of EGFR tyrosine kinase inhibitors in the first-line treatment of advanced non small cell lung cancer patients harboring EGFR mutation. Curr. Med. Chem. 19, 3337–3352.

Sherman, W., Beard, H.S., Farid, R., 2006a. Use of an induced fit receptor structure in virtual screening. Chem. Biol. Drug Des. 67, 83–84.

Sherman, W., Day, T., Jacobson, M.P., Friesner, R.A., Farid, R., 2006b. Novel procedure for modeling ligand/receptor induced fit effects. J. Med. Chem. 49, 534–553.

Soonthornthum, T., Arias-Pulido, H., Joste, N., Lomo, L., Muller, C., Rutledge, T., Verschraegen, C., 2011. Epidermal growth factor receptor as a biomarker for cervical cancer. Ann. Oncol. 22, 2166–2178.

Sugiura, Y., Nemoto, E., Kawai, O., Ohkubo, Y., Fusegawa, H., Kaseda, S., 2013. Gefitinib frequently induces liver damage in patients with lung adenocarcinoma previously treated by chemotherapy. Lung Cancer: Targets Ther. 4, 9–14.

Sun, J.Z., Lu, Y., Xu, Y., Liu, F., Li, F.Q., Wang, Q.L., Wu, C.T., Hu, X.W., Duan, H.F., 2012. Epidermal growth factor receptor expression in acute myelogenous leukaemia is associated with clinical prognosis. Hematol. Oncol. 30, 89–97.

Tebbutt, N., Pedersen, M.W., Johns, T.G., 2013. Targeting the ERBB family in cancer: couples therapy. Nat. Rev. Cancer 13, 663–673.

Traxler, P., 2003. Tyrosine kinases as targets in cancer therapy – successes and failures. Expert Opin. Ther. Targets 7, 215–234.

Traxler, P., Allegrini, P.R., Brandt, R., Brueggen, J., Cozens, R., Fabbro, D., Grosios, K., Lane, H.A., McSheehy, P., Mestan, J., Meyer, T., Tang, C., Wartmann, M., Wood, J., Caravatti, G., 2004. AEE788: a dual family epidermal growth factor receptor/ErbB2 and vascular endothelial growth factor receptor tyrosine kinase inhibitor with antitumor and antiangiogenic activity. Cancer Res. 64, 4931–4941.

Ullrich, A., Coussens, L., Hayflick, J.S., Dull, T.J., Gray, A., Tam, A.W., Lee, J., Yarden, Y., Libermann, T.A., 1984. Human epidermal growth factor receptor cDNA sequence and aberrant expression of the amplified gene in A431 epidermoid carcinoma cells. Nature 309, 418–425.

Wilson, M.B., Schreiner, S.J., Choi, H.J., Kamens, J., Smithgall, T.E., 2002. Selective pyrrolo-pyrimidine inhibitors reveal a necessary role for Src family kinases in Bcr–Abl signal transduction and oncogenesis. Oncogene 21, 8075–8088.

Wu, Y.J., Davis, C.D., Dworetzky, S., Fitzpatrick, W.C., Harden, D., He, H., Knox, R.J., Newton, A.E., Philip, T., Polson, C., Sivarao, D.V., Sun, L.Q., Tertyshnikova, S., Weaver, D., Yeola, S., Zoeckler, M., Sinz, M.W., 2003. Fluorine substitution can block CYP3A4 metabolism-dependent inhibition: identification of (S)-N-[1-(4-fluoro-3-morpholin-4-ylphenyl)ethyl]-3-(4-fluorophenyl)acrylamide as an orally bioavailable KCNQ2 opener devoid of CYP3A4 metabolism-dependent inhibition. J. Med. Chem. 46, 3778–3781.

Wu, Y.L., Lee, J.S., Thongprasert, S., Yu, C.J., Zhang, L., Ladrera, G., Srimuninnimit, V., Sriuranpong, V., Sandoval-Tan, J., Zhu, Y., Liao, M., Zhou, C., Pan, H., Lee, V., Chen, Y.M., Sun, Y., Margono, B., Fuerte, F., Chang, G.C., Seetalarom, K., Wang, J., Cheng, A., Syahruddin, E., Qian, X., Ho, J., Kurnianda, J., Liu, H.E., Jin, K., Truman, M., Bara, I., Mok, T., 2013. Intercalated combination of chemotherapy and erlotinib for patients with advanced stage non-small-cell lung cancer (FASTACT-2): a randomised, double-blind trial. Lancet Oncol. 14, 777–786.

Xu, J., Escamilla, J., Mok, S., David, J., Priceman, S., West, B., Bollag, G., McBride, W., Wu, L., 2013. CSF1R signaling blockade stanches tumor-infiltrating myeloid cells and improves the efficacy of radiotherapy in prostate cancer. Cancer Res. 73, 2782–2794.

Yarden, Y., Pines, G., 2012. The ERBB network: at last, cancer therapy meets systems biology. Nat. Rev. Cancer 12, 553–563.

Yoshida, T., Yamada, K., Azuma, K., Kawahara, A., Abe, H., Hattori, S., Yamashita, F., Zaizen, Y., Kage, M., Hoshino, T., 2013. Comparison of adverse events and efficacy between gefitinib and erlotinib in patients with non-small-cell lung cancer: a retrospective analysis. Med. Oncol. 30, 1–7.

Yun, C.H., Boggon, T.J., Li, Y., Woo, M.S., Greulich, H., Meyerson, M., Eck, M.J., 2007. Structures of lung cancer-derived EGFR mutants and inhibitor complexes: mechanism of activation and insights into differential inhibitor sensitivity. Cancer Cell 11, 217–227.

Please cite this article in press as: Kaspersen, S.J., et al. Identification of new 4-*N*-substituted 6-aryl-7*H*-pyrrolo[2,3-*d*] pyrimidine-4-amines as highly potent EGFR-TK inhibitors with Src-family activity. Eur. J. Pharm. Sci. (2014), http://dx.doi.org/10.1016/j.ejps.2014.04.011